

Slow charge recombination in dye-sensitised solar cells (DSSC) using Al_2O_3 coated nanoporous TiO_2 films

Emilio Palomares, John N. Clifford, Saif A. Haque, Thierry Lutz and James R. Durrant*

Centre for Electronic Materials and Devices, Department of Chemistry, Imperial College of Science, Technology and Medicine, Exhibition Road, London, UK SW7 2AY. E-mail: j.durrant@ic.ac.uk

Received (in Cambridge, UK) 13th March 2002, Accepted 17th May 2002

First published as an Advance Article on the web 7th June 2002

The conformal growth of an overlayer of Al_2O_3 on a nanocrystalline TiO_2 film is shown to result in a 4-fold retardation of interfacial charge recombination, and a 30% improvement in photovoltaic device efficiency.

In the last decade, dye-sensitised solar cells (DSSC) have been developed into one of the most interesting alternatives to current solar cell technology for the conversion of sunlight into electrical energy.¹

A typical DSSC comprises a dye sensitised porous, nanocrystalline titanium dioxide film interpenetrated by a liquid electrolyte containing an I^-/I_3^- red/ox couple. The main charge-transfer events taking place at the TiO_2 /dye/electrolyte interface are depicted in Scheme 1. Visible light is absorbed (1) by the sensitiser dye (e.g.: $\text{RuL}_2(\text{SCN})_2$ where L is 4,4'-dicarboxy-2,2'-bipyridyl). Electron injection (2) from the excited state of the dye into the conduction band of the TiO_2 is followed by the subsequent regeneration of the dye by the I^-/I_3^- red/ox couple (4).

Efficient operation of the DSSC device relies upon the minimisation of the possible recombination pathways occurring at the TiO_2 /dye/electrolyte interface, allowing efficient charge transport through the TiO_2 film and electrolyte and subsequent charge collection at the device contacts. There are two possible recombination losses to consider. The injected electrons may recombine either with oxidized dye molecules (3) or with the oxidised redox couple (5); the latter reaction is thought to be particularly critical to device function.

Increasingly research into DSSC is addressing the use of more sophisticated device architectures in order to reduce interfacial recombination losses. Examples include the use of composite metal oxides as the semiconductor e.g. SnO , ZnO with different band-gaps,² the incorporation of spacer units between the oxidised dye and the TiO_2 surface,⁴ and surface passivation by electrodeposition of insulating polymers.⁵ One particularly attractive approach involves the coating of the nanocrystalline metal oxide film with a thin overcoat of another metal oxide with a higher conduction band edge, as illustrated in Scheme 1, with the aim of increasing the physical separation of injected electrons for the oxidised dye redox couple, thereby

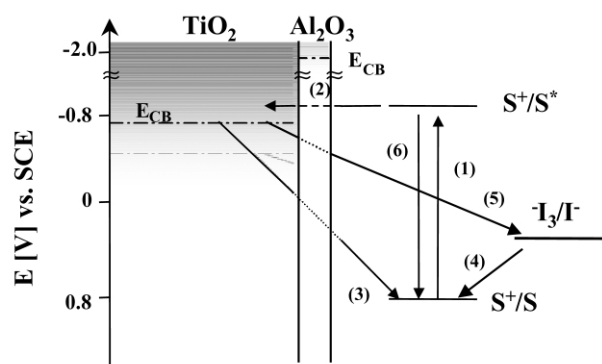
retarding the recombination reactions. Previous studies employing this approach have demonstrated significant improvements in DSSC device performance for Nb_2O_5 coated TiO_2 films and Al_2O_3 coated SnO_2 films.^{6,7}

In this paper we employ transient laser spectroscopy to probe directly the retardation of interfacial charge recombination caused by coating a nanocrystalline TiO_2 with an Al_2O_3 overlayer. We moreover suggest the simplicity of the coating method presented, may make this approach particularly attractive for the future development of efficient DSSC.

Al_2O_3 coated nanocrystalline TiO_2 films were prepared by the following method. An 8 μm thick porous film of nanocrystalline, anatase TiO_2 was deposited by the doctor blade technique onto fluorine doped conducting tin oxide glass (TEC8) (nanocrystal diameter ~ 15 nm) as previously.⁸ An air-stable solution of $\text{Al}(\text{Bu}^i\text{O})_3$ (Sigma-Aldrich[®], 99.9% grade, 0.15 M in isopropanol) under aerobic conditions was used to conformally coat the TiO_2 . The film was exposed to water vapour for 1 min and dried at 120 $^\circ\text{C}$. After this, the film was dipped in the coating solution for 15 min at 60 $^\circ\text{C}$ and, finally, sintered at 450 $^\circ\text{C}$ for 15 min in order to remove any remaining organic contaminants. HRTEM data (data to be presented elsewhere) indicate this procedure resulted in a conformal Al_2O_3 overlayer with thickness of ~ 2 –2.5 nm. After coating, the samples were sensitised under anhydrous conditions by a standard solution of dye $\text{RuL}_2(\text{NCS})_2^{\dagger}$ overnight at room temperature, resulting in similar dye loadings for both films (see Table 1).

The influence of this coating procedure upon the kinetics of the recombination reaction (3) was determined using millisecond–microsecond transient absorption spectroscopy, monitoring the decay of photoinduced absorption of the dye cation species in the absence of a red/ox active electrolyte. Data were collected with the sensitised film covered in a 1:1 ethylene carbonate/propylene carbonate solution and glass cover slide following previously published methods.⁹ Fig. 1 contrasts the decay kinetics plotted on a logarithmic time scale in the presence and absence of the Al_2O_3 overcoat on the TiO_2 film. The charge recombination kinetics exhibits the previously reported¹⁰ stretched-exponential behaviour ($\Delta OD \propto e^{-(t/\tau)^\alpha}$). It is apparent that the Al_2O_3 overlayer results in a ~ 4 fold retardation of the recombination (half times for dye cation decay of 2.0 and 0.57 ms for the coated and uncoated films, respectively), consistent with the blocking layer function of the Al_2O_3 overlayer.

The recombination data shown in Fig. 1 are consistent with a reasonably homogeneous Al_2O_3 overlayer thickness. An inhomogeneous overcoat would be expected to result in more



Scheme 1 Illustration of the interfacial charge-transfer processes occurring at the nanostructured TiO_2 /dye/electrolyte interface of DSSC. Also shown is the Al_2O_3 blocking layer as developed in this paper.

Table 1 Comparison of the performance parameters of the cells based on $\text{Al}_2\text{O}_3/\text{TiO}_2$ and TiO_2 films

	V_{OC}/mV	J_{SC}/mA	FF (%)	η (%)
$\text{Al}_2\text{O}_3/\text{TiO}_2^a$	750	10.9	65	5
TiO_2^b	705	8.1	55	3.8

^a Absorbance of dye-coated film was 2.28. ^b Absorbance of dye-coated film was 2.30 measured at 550 nm.



Fig. 1 Transient absorption data probing the decay of photoinduced dye cation absorption (excitation 625 nm, probe 800 nm) at room temperature for (a) an $\text{Al}_2\text{O}_3/\text{TiO}_2/\text{RuL}_2(\text{NCS})_2$ film and (b) a $\text{TiO}_2/\text{RuL}_2(\text{NCS})_2$ film. The decay dynamics are assigned to the recombination reaction (3) in Scheme 1.

dispersive (*i.e.* more stretched) recombination kinetics, whereas we observe the coating actually results in less dispersive kinetics (as will be discussed in more detail elsewhere). We furthermore note that coated films exhibited a similar initial signal amplitude to the uncoated films, indicative of similar electron injection yields for both films. This observation is consistent with previous studies¹¹ of uncoated films which have reported that the rate of the electron injection reaction (2) is $>10^3$ greater than the excited state decay reaction (6), indicating the injection yield would be insensitive to a four-fold reduction in the rate of electron injection.

The influence of the Al_2O_3 overlayer on photovoltaic performance was investigated by the fabrication of a 1 cm^2 'sandwich' DSSC.[‡] Photoelectrochemical measurements were performed according to reported procedures.

Fig. 2 illustrates the photocurrent–voltage curves for cells with and without blocking-layer of Al_2O_3 . Open circuit voltage



Fig. 2 Photocurrent–voltage curves of DSSC with (a) and without (b) the incorporation of an Al_2O_3 overlayer under AM 1.5 irradiation. The inset illustrates the dark current in both samples.

(V_{OC}), short circuit photocurrent density (J_{SC}), fill factor (FF), and photoenergy conversion efficiency (η) of the cells are listed in Table 1. We conclude that the Al_2O_3 overlayer results in a significant improvement in V_{OC} , I_{SC} and FF, with an overall 30% improvement in device performance. The improvement in cell voltage is of particular relevance. It should be noted that the control (no overlayer) cells employed in these studies were optimised for compatibility with transient spectroscopy rather than device efficiency. As shown elsewhere, further improvements in device performance should be obtained by the use of scattering metal oxide films, reflective counter electrodes, and reduction in series resistance losses from the electrodes and electrolyte.

The dark current data in Fig. 2 (see insert) indicates that the Al_2O_3 overlayer reduces the dark current arising from the recombination reaction (5) in Scheme 1. This is consistent with the observed 45 mV increase in V_{OC} of the device under illumination and provides further support for the blocking layer function of the Al_2O_3 overlayer. In addition we find this overlayer results in a significant increase in I_{SC} , as has been previously reported for Nb_2O_5 overlayers.⁶ This observation may in part be attributed to an increase in the yield of electron injection, as we discuss above. It may also arise from other factors such as an improvement in electron transport through the metal oxide, as has previously been discussed in relation to TiCl_4 treatments of such films.¹²

In conclusion we have demonstrated a simple method for the fabrication of conformal Al_2O_3 overlayer on nanocrystalline TiO_2 films, have demonstrated that this overlayer results in a retardation of the kinetics of charge recombination to dye cations (reaction (3)) and a reduction in the dark current (reaction (5)), resulting in 30% overall improvement in device performance under solar illumination.

We gratefully acknowledge the support of the EPSRC and the European Union (Nanamax, NNE5-2001-00192) in funding this research.

Notes and references

† Chemical name: *cis*-bis(isothiocyanato)bis(2,2'-bipyridyl-4,4'-dicarboxylato)ruthenium(II) bis-tetrabutylammonium.

‡ The electrolyte solution contains 2.216 g of tetrabutylammonium iodide (0.6 M), 0.134 g LiI (0.1 M), 0.253 g I_2 (0.1 M) and 0.676 g 4-*tert*-butylpyridine (0.5 M) in 10 ml of acetonitrile. The counter electrode was made using a solution of chloroplatinic acid (1 g of acid in 40 ml of isopropanol).

- B. O'Regan and M. Grätzel, *Nature*, 1999, **353**, 737.
- K. Tennakone, V. P. S. Perera, I. R. M. Kottegoda and G. R. A. Kum, *J. Phys. D: Appl. Phys.*, 1999, **32**, 374.
- M. K. Nazeeruddin, A. Kay, I. Rodicio, R. Baker Humphry, E. Muller, P. Liska, N. Vlachopoulos and M. Grätzel, *J. Am. Chem. Soc.*, 1993, **115**, 6382.
- R. Argazzi, C. A. Bignozzi, T. A. Heimer and G. J. Meyer, *Inorg. Chem.*, 1997, **36**, 2.
- B. A. Gregg, F. Pichot, S. Ferrere and C. L. Fields, *J. Phys. Chem. B.*, 2001, **105**, 1422.
- A. Zaban, S. G. Chen, S. Chappel and B. A. Gregg, *Chem. Commun.*, 2000, 2231.
- G. R. R. A. Kummara, K. Tennakone, V. P. S. Perera, V. A. Kono, S. Kaneko and M. Okuya, *J. Phys. D: Appl. Phys.*, 2001, **34**, 868.
- R. L. Willis, C. Olson, B. O'Regan, T. Lutz, J. Nelson and J. R. Durrant, *J. Phys. Chem. B*, 2002, in press.
- S. A. Haque, Y. Tachibana, R. L. Willis, J. E. Moser, M. Grätzel, D. R. Klug and J. R. Durrant, *J. Phys. Chem. B*, 2000, **104**, 538.
- S. A. Haque, Y. Tachibana, D. R. Klug and J. R. Durrant, *J. Phys. Chem. B*, 1998, **102**, 1745.
- Y. Tachibana, J. E. Moser, M. Grätzel, D. R. Klug and J. R. Durrant, *J. Phys. Chem.*, 1996, **100**, 20056.
- N.-G. Park, J. Schlichthorl, H. M. van de Lagemaat, A. Cheong, A. J. Mascarenhas and J. Frank, *J. Phys. Chem. B*, 1999, **103**, 3308.